Journal of Hazardous Materials 192 (2011) 1140–1147

Contents lists available at ScienceDirect

Journal of Hazardous Materials

journal homepage: www.elsevier.com/locate/jhazmat

Magnetic mesoporous materials for removal of environmental wastes

Byoung Chan Kim[a], Jinwoo Lee[b], Wooyong Um[c], Jaeyun Kim[d], Jin Joo[e], Jin Hyung Lee[f], Ja Hun Kwak[c], Jae Hyun Kim[g], Changha Lee[h], Hongshin Lee[h], R. Shane Addleman[c], Taeghwan Hyeon[d], Man Bock Gu[i,**], Jungbae Kim[g,*]

[a] Environment Sensor System Research Center, Korea Institute of Science and Technology, Seoul 136-791, Republic of Korea
[b] Department of Chemical Engineering, Pohang University of Science and Technology, San 31, Hyo-ja dong, Pohang, 790-784, Republic of Korea
[c] Pacific Northwest National Laboratory, Richland, WA 99352, USA
[d] National Creative Research Initiative Center for Oxide Nanocrystalline Materials, School of Chemical and BiologicalEngineering, Seoul National University, Seoul 151-744, Republic of Korea
[e] Department of Applied Chemistry, Kyungpook National University, Daegu 702-701, Republic of Korea
[f] Korea Institute of Ceramic Engineering and Technology, Seoul 153-801, Republic of Korea
[g] Department of Chemical and Biological Engineering, Korea University, Seoul 136-701, Republic of Korea
[h] School of Urban and Environmental Engineering, Ulsan National Institute of Science and Technology (UNIST), Ulsan 689-798, Republic of Korea
[i] College of Life Sciences and Biotechnology, Korea University, Seoul 136-701, Republic of Korea

ARTICLE INFO

Article history:
Received 21 July 2010
Received in revised form 9 June 2011
Accepted 9 June 2011
Available online 17 June 2011

Keywords:
Magnetic mesoporous materials
Adsorption
Mercury
Tyrosinase
Catehcol degradation

ABSTRACT

We have synthesized two different magnetic mesoporous materials that can be easily separated from aqueous solutions by applying a magnetic field. Synthesized magnetic mesoporous materials, Mag-SBA-15 (magnetic ordered mesoporous silica) and Mag-OMC (magnetic ordered mesoporous carbon), have a high loading capacity of contaminants due to high surface area of the supports and high magnetic activity due to the embedded iron oxide particles. Application of surface-modified Mag-SBA-15 was investigated for the collection of mercury from water. The mercury adsorption using Mag-SBA-15 was rapid during the initial contact time and reached a steady-state condition, with an uptake of approximately 97% after 7 h. Application of Mag-OMC for collection of organics from water, using fluorescein as an easily trackable model analyte, was explored. The fluorescein was absorbed into Mag-OMC within minutes and the fluorescent intensity of solution was completely disappeared after an hour. In another application, Mag-SBA-15 was used as a host of tyrosinase, and employed as recyclable catalytic scaffolds for tyrosinase-catalyzed biodegradation of catechol. Crosslinked tyrosinase in Mag-SBA-15, prepared in a two step process of tyrosinase adsorption and crosslinking, was stable enough for catechol degradation with no serious loss of enzyme activity. Considering these results of cleaning up water from toxic inorganic and organic contaminants, magnetic mesoporous materials have a great potential to be employed for the removal of environmental contaminants and potentially for the application in large-scale wastewater treatment plants.

1. Introduction

Human activities generate a large quantity of various pollutants into the environment. Many places are contaminated by heavy metals, organic compounds and other hazardous materials, which deleteriously impact the ecosystem. In recent years, many researchers have investigated a range of innovative techniques for the efficient removal of contaminants from polluted water. Remediation techniques for water treatment can be categorized into biological, chemical and physical treatment methods [1]. For example, various techniques such as biodegradation, electron-beam irradiation, extraction, adsorption, air sparging and incineration are being used to remove or reduce the contaminants in water [2,3]. Especially, the adsorption of contaminants is broadly employed in the field due to the simplicity and economics of this approach. The removal efficiency by adsorption is mostly determined by the properties of an adsorbent, and several materials have been used as adsorbents, such as activated carbons [4,5], zeolites [6,7], iron oxides [8,9] and silica [10].

* Corresponding author at: Department of Chemical and Biological Engineering, Korea University, Seoul 136-701, Republic of Korea. Tel.: +82 2 3290 4850; fax: +82 2 926 6102.
** Corresponding author at: College of Life Sciences and Biotechnology, Korea University, Seoul 136-701, Republic of Korea. Tel.: +82 2 3290 3417; fax: +82 2 928 6050.
E-mail addresses: mbgu@korea.ac.kr (M.B. Gu), jbkim3@korea.ac.kr (J. Kim).

0304-3894/$ – see front matter © 2011 Elsevier B.V. All rights reserved.
doi:10.1016/j.jhazmat.2011.06.022

Mesoporous materials have been synthesized for a variety of applications involving large molecules; such applications cannot be accomplished using conventional microporous zeolitic materials [11–14]. Various other organic templates including neutral amine surfactants [15,16], alkyl polyethylene oxide (PEO) surfactants [17], and triblock copolymers [18] have been used for the synthesis of mesostructured silica materials with diverse pore structures. Particularly, large sized SBA-15 [18] mesoporous silica, synthesized using triblock copolymers, has attracted much attention in the society of catalyses, biotechnology, and environmental waste treatment. The application of Self Assembled Monolayers on Mesoporous Supports (SAMMS) technology to environmental remediation is gathering a lot of attention because SAMMS based adsorption enables fast kinetics, high material loading and good selectivity based on the surface functionalization and large surface area. Many studies have reported that the SAMMS particles were successfully utilized for removal of various heavy metals from the waste solution [19–23]. The SAMMS are organosilicate sorbent materials and post processing recovery or separation of SAMMS is feasible by using filtration or centrifugation, but those are not suitable for large-scale industrial plants. In addition, the SAMMS particles, themselves, might cause secondary environmental contamination if they are not fully recovered from environment. It has been warned that engineered nanomaterials may have different properties from original substances [24]. Consequently nanomaterials may be harmful to the biosphere although original substances cause no toxicity. Therefore, the facile separation of nanosturctured sorbents is very important in their industrial applications in order not to make a harmful impact to the environment.

In the present work, we report the synthesis of magnetically separable mesoporous materials and their applications for the removal of environmental contaminants from aquatic system. Two types of magnetic mesoporous materials, Mag-SBA-15 (magnetic ordered mesoporous silica) and Mag-OMC (magnetic ordered mesoporous carbon), were synthesized as magnetically separable high surface area support structures for remediation efforts. These materials were modified and used for the removal of mercury, an adsorption of an organic dye, and the biodegradation of catechol by the immobilized enzyme tyrosinase. These materials could be easily separated from water by using a magnet, and the removal of contaminants was effective due to high affinity to target contaminants on their appropriately functionalized large surface. Magnetic mesoporous materials can be potentially employed as recoverable adsorbents in large-scale plants of waste water treatment due to their facile separation and high adsorption capacity [25–29].

2. Materials and methods

2.1. Preparation of magnetically separable SBA-15 mesoporous silica and magnetically separable ordered mesoporous carbon

Pristine SBA-15 silica was prepared by following a reported procedure (Fig. S1a in supplementary data) [18]. Briefly, 4 g of P123 (BASF, poly(ethylene oxide)$_{20}$-poly(propylene oxide)$_{70}$-poly(ethylene oxide)$_{20}$) was dissolved in solution composed of 130 mL deionized water and 20 mL hydrochloric acid (37 wt%), and the temperature of the solution was raised to 40 °C. TEOS (9.2 mL) was added to the solution and stirred vigorously and the solution was remained at 40 °C for 20 h, followed by aging at 100 °C for 24 h. The resulting material was put in a beaker and reacted at 100 °C for 24 h. The resultant white precipitate was filtered, dried at room temperature and finally calcined at 550 °C to remove P123. By thermal decomposition [30] of Fe-carboxylate coordinate composite, magnetic nanoparticles were deposited into montmorillonites [31], fumed silica [32], and MCM-41 [33]. In the present work, 1.34 g $Fe(NO_3)_3{\cdot}9H_2O$ in 3 mL methanol was impregnated into 0.5 g SBA-15 silica, and dried in a oven at 85 °C till the methanol was completely dried. The $Fe(NO_3)_3$ impregnated silica was reacted with propionic acid vapor at 85 °C for more than 3 h under static vacuum to make iron propionate complex. The composite was heated to 300 °C under air (1 °C min^{-1}) slowly for decomposition of iron propionate complex, and kept at 300 °C for 30 min. The resulting magnetic nanoparticle incorporated SBA-15 is denoted as Mag-SBA-15 (magnetically separable SBA-15).

For the thiol (-SH) functionalization, 1 g of Mag-SBA-15 was suspended in 100 mL of anhydrous toluene, and refluxed for 3 h. The stoichiometric amount of 3-mercaptopropyltriethoxysilane was added and refluxed overnight. After cooling to room temperature, the mixture was filtered and washed thoroughly with toluene, and dried under vacuum. The triethoxy groups of mecaptopropyltriethoxysilane can be hydrolyzed into three silanol groups, which can react with free silanol groups on the surface of mesoporous silica. By this simple condensation, mercaptopropyl group containing thiol (-SH) functional group can be anchored on the surface of mesoporous silica [34,35].

Mag-OMC was prepared by following the reported procedure (Fig. S1b in supplementary data) [36]. Briefly, pyrrole monomer, based on the pore volume of SBA-15, was incorporated into SBA-15 by vapor phase infiltration under static vacuum. The resulting pyrrole/SBA-15 nanocomposite was dispersed in H_2O containing 2.3 molar equivalents of $FeCl_3$ to the amount of pyrrole, and stirred for 3 h to polymerize the pyrrole inside the mesoporous SBA-15 silica template. After recovering the poly(pyrrole)/SBA-15 nanocomposite by filtration, it was carbonized in a N_2 atmosphere at 800 °C for 3 h. The silica template was removed by boiling the silica/carbon composite in 1 M NaOH solution, and dissolved in 50:50 mixture (v:v) of water and ethanol for more than 1 h twice.

2.2. Magnet capture of porous magnetic nanoparticles

For magnetic separation of Mag-SBA-15 or Mag-OMC, these porous magnetic nanoparticles were dispersed in 10 mM sodium phosphate buffer (pH 7.0) by vortexing and further sonication for 30 s. Suspended nanoparticles were transferred in glass vials. To examine cyclic recovery performance of porous magnetic nanoparticles, glass vials containing Mag-SBA-15 (0.5 mg mL^{-1}) or Mag-OMC (0.5 mg mL^{-1}) were attached on a magnet for 60 min at least and recovered particles were resuspended. At each cyclic step, solution after magnet capturing was taken and residual particles in solution were observed using UV spectrophotometer (Cary 5G, Varian, Inc.) at A320 nm.

2.3. Hg adsorption

The synthesized materials with magnetic property were used as adsorbents in the mercury adsorption study. NANOpure™ water (high-purity water of at least 18 MΩ cm resistivity) was used for preparing all solutions. Mercury (Hg(II)) was added as mercury nitrate ($Hg(NO_3)_2$) (Aldrich). Sodium nitrate ($NaNO_3$) was used to adjust the ionic strength of the background electrolyte, and the pH of the solution was adjusted using nitric acid (HNO_3) or sodium hydroxide (NaOH). Batch adsorption experiments were conducted in individual 15 mL polypropylene centrifuge tubes by mixing the thiol functionalized Mag-SBA-15 with a Hg(II) solution. Various initial Hg(II) concentrations ranging from 2.0 to 790 mg L^{-1} and a constant solid concentration of 1 g L^{-1} were used in the experiments. All experiments were conducted in closed test tubes with a minimal headspace, and a CO_2-free solution

(N_2-sparged NANOpure™ water) was used to prepare all solutions to minimize CO_2(g) absorption. The Hg(II) solution with a constant background electrolyte (I = 0.01 M $NaNO_3$) was added to the test tubes containing the adsorbents. Test tubes without adsorbents were also prepared in an identical manner to determine the initial Hg(II) concentration and to ensure that there was no Hg(II) adsorption to the container walls. The test tubes were placed on a slow-moving platform shaker for 24 h. The 24 h period was based on the results of a suite of kinetic experiments conducted previously to determine Hg(II) adsorption uptake as a function of time. Each of several separate test tubes was prepared using the same experimental conditions as described, and one tube at a specific time was periodically removed for analysis. The results of kinetic experiments showed that 1 day was sufficient to reach steady-state conditions. Generally, more rigorous mixing improved the mass transport and reduced time to equilibrium. After equilibrium, the magnet was used to separate the solution from the adsorbents. The final pH was measured, and a 2 mL aliquot was removed from the supernatant solution for Hg(II) analysis. The Hg(II) concentration was determined by inductively coupled plasma mass spectroscopy (ICP-MS, Perkin Elmer Inc., Wellesley, MA). Fractional sorption uptake was calculated as a difference between the initial and the final Hg(II) concentrations. The values of distribution coefficient, K_d (mL g^{-1}), were calculated using the difference between initial and final concentrations in solution to represent the concentration of Hg(II) adsorbed to the adsorbents.

2.4. Fluorescein adsorption

Fluorescent dye, fluorescein ($C_{20}H_{12}O_5$, Sigma–Aldrich), was dissolved in *N,N*-dimethylformamide, and this stock solution was diluted to 10 mM sodium phosphate buffer (pH 7.0). The adsorption of fluorescein was performed by adding Mag-OMC (40 mg) into fluorescein solution (10,000 ppm, 3 mL), and the vial was shaken at 250 rpm. After 60 min, the glass vial was attached on the magnet for 40 min. Residual fluorescent intensity in solution was measured at 512 nm emission after excitation at 492 nm using spectrofluorophotometer (RF5301-PC, Shimadzu, Japan) before and after adsorption of fluorescein.

2.5. Tyrosinase entrapped Mag-SBA-15 and its uses for catechol oxidation

For adsorption of tyrosinase (TY, Sigma–Aldrich), 10 mg of Mag-SBA-15 was mixed with 1.5 mL of 4 mg mL^{-1} TY solution in 100 mM sodium phosphate buffer (pH 6.5), vortexed for 30 s, sonicated for 5 s, and incubated at room temperature under shaking (250 rpm) for 30 min. After incubation, the samples were washed briefly with 100 mM sodium phosphate buffer (pH 6.5), and further treated with 0.1% glutaraldehyde (GA) solution in 100 mM sodium phosphate buffer (pH 8.0) at 200 rpm for 30 min to achieve the nanoscale enzyme reactors of TY (NER-TY) in Mag-SBA-15. After GA treatment, the samples were washed by 100 mM sodium phosphate buffer (pH 8.0) and 100 mM Tris-HCl buffer (pH 8.0). The capping of unreacted aldehyde groups was performed in a fresh 100 mM Tris-HCl buffer (pH 8.0) at 200 rpm for 30 min. After capping, the samples were washed five times by using 100 mM sodium phosphate buffer (pH 6.5) and stored at 4 °C. The adsorbed TY (ADS-TY) was also prepared by omitting the GA treatment, but the washing was performed in an exactly same way as for NER-YT.

The TY activity was determined by oxidation of 1 mM catechol in an aqueous buffer (100 mM sodium phosphate buffer, pH 6.5) at room temperature under rigorous shaking (250 rpm), which could be measured by checking the increase of absorbance at 394 nm. The stabilities of ADS-TY and NER-TY were investigated by incubating each sample in 100 mM sodium phosphate buffer (pH 6.5) under rigorous shaking (250 rpm) and checking the residual activity. At each cycle, the suspended samples were captured by using a magnet, the solution was decanted, the same volume of fresh sodium phosphate buffer was added to the suspension, and excessive washing was finally performed under the shaking condition (250 rpm) for 1 h. This procedure was repeated for 30 cycles, and the residual activities were measured after 0, 5, 10, 15, 20, 25, and 30 cycles. The relative activity was calculated from the ratio of the residual activity to the initial activity of each sample.

3. Results and discussion

3.1. Synthesize of Mag-SBA-15 and Mag-OMC

Mag-SBA-15 was synthesized by the thermal decomposition of iron propionate complex formed by reaction between Fe^{3+} salt and propionic acid. During the decomposition and conversion of iron propionate to magnetic nanoparticles, the formed nanoparticles extruded from the mesopores, which resulted in the formation of hierarchical magnetic nanoparticle assembly outside the pores (Figs. 1a and 2a). Due to the magnetic nanoparticles formed outside the pores, the mesoporous silica Mag-SBA-15 could be effectively separated by using a magnet. The growth of nanoparticles outside the pores were reported by two groups [37,38]. Silver superstructure was formed outside the pores of MCM-48 [37]. The

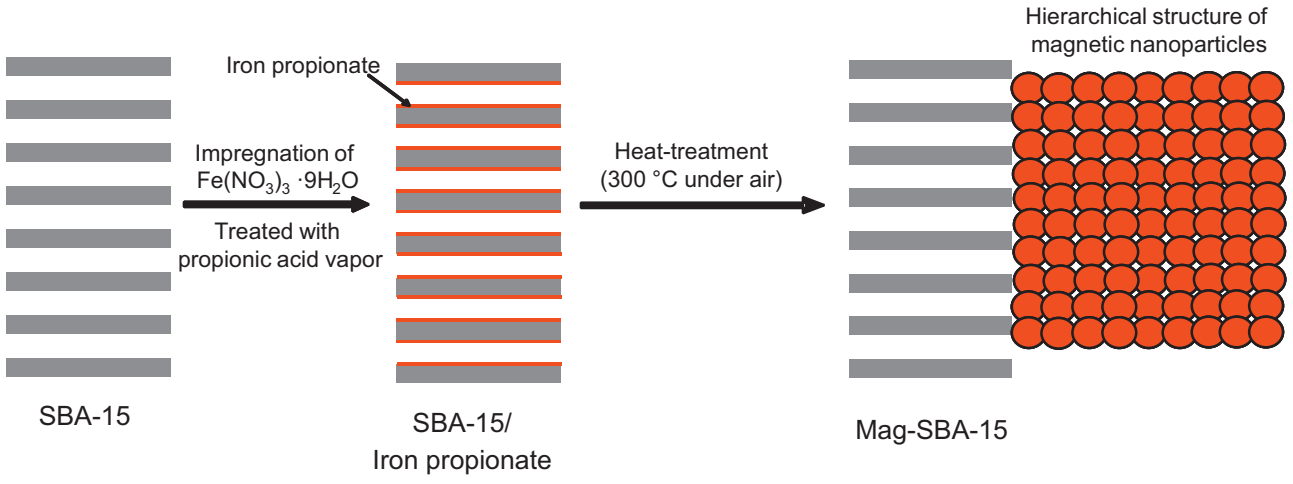

Fig. 1. Schematic representation for the formation of hierarchically magnetic nanoparticle assembly outside the pores of SBA-15.

impregnated $AgNO_3$ was converted to Ag nanoparticles at high temperature (300 °C) in the pores and subsequently assembled into the superstructure on the surface of MCM-48 particles. They claimed that huge free excess energy in nanoparticles made the nanoparticle mobile, resulting in the superstructure of nanoparticle aggregates. During the formation of superstructure, the ordered channels of MCM-48 guided the assembly into ordered structures. In a similar way, palladium superstructures were also formed outside the MCM-48 particles [38].

Schüth group also reported magnetically separable mesoporous silica, which were synthesized in a multi-step process [39]. They first prepared magnetic nanoparticles via a high-temperature thermal decomposition method, filled up all the mesopores with thermally decomposable polymer, adsorbed magnetite nanoparticles onto the surface of mesoporous silica particles, and carbonized furfuryl alcohol to prevent the leaching of magnetic nanoparticles from the surface of mesostructured silica [39]. However, the present work adopted a simpler approach for the synthesis of

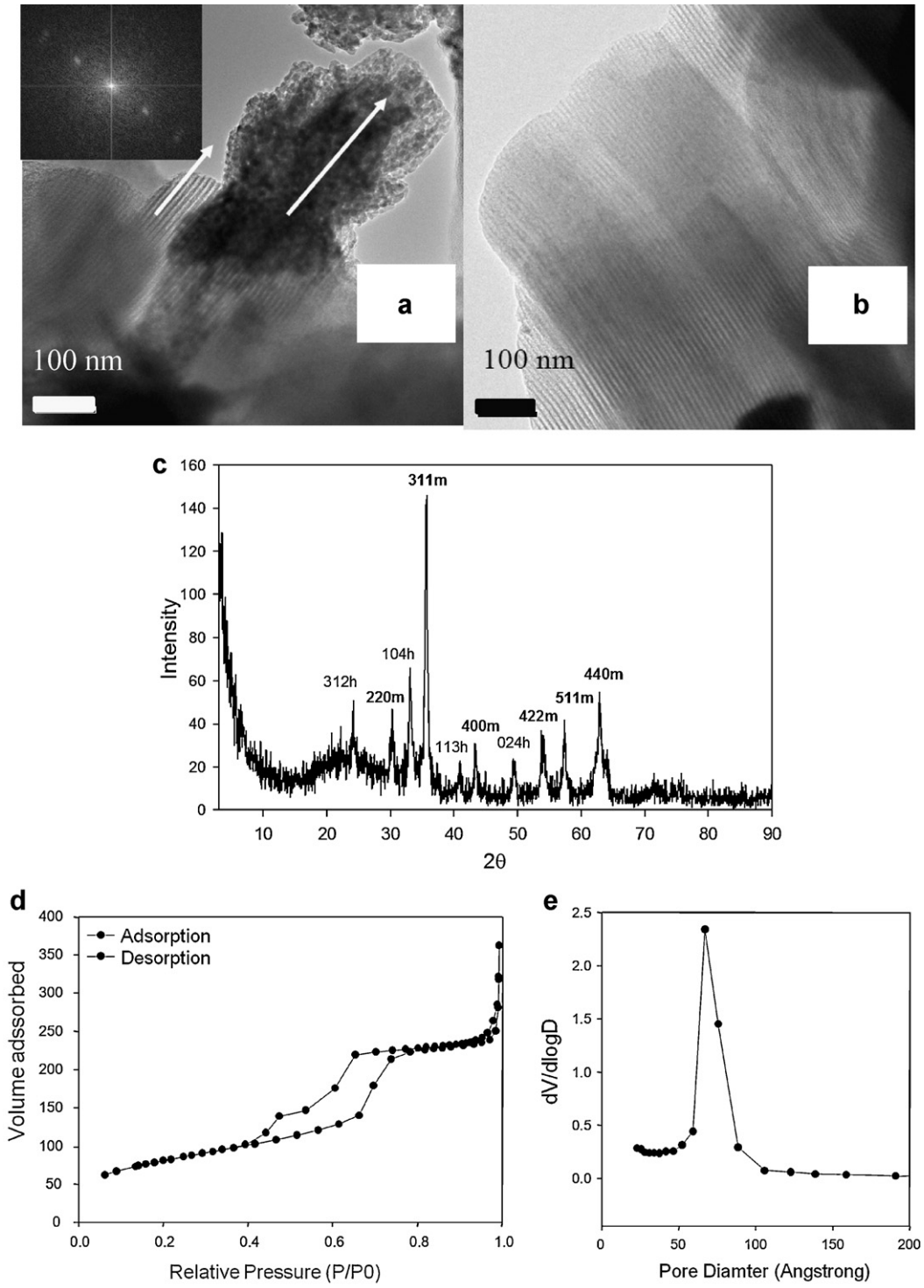

Fig. 2. (a) TEM image of Mag-SBA-15, (inset) Fourier transformation pattern of Mag-SBA-15; (b) TEM image of Mag-SBA-15 obtained at the opposite site from the hierarchically formed magnetic nanoassembly; (c) XRD pattern of Mag-SBA-15; (d) Nitrogen isotherms of Mag-SBA-15; (e) pore size distribution of Mag-SBA-15 obtained from adsorption isotherm. The scale bar of (a) and (b) denotes 100 nm.

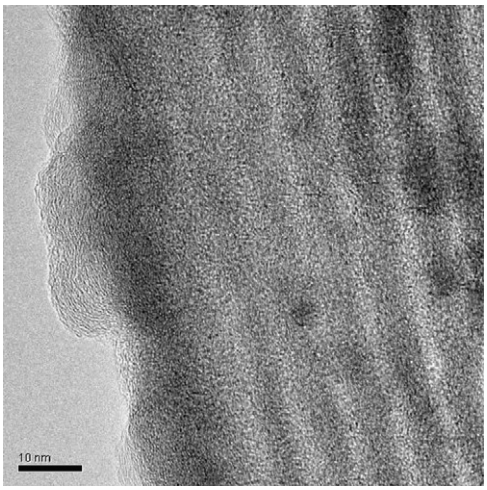

Fig. 3. A representative TEM image of Mag-OMC.

open-pore magnetic silica SBA-15 without using preformed magnetic nanoparticle. Fourier transformation pattern of Mag-SBA-15 reveals the hexagonally ordered regular array of pores. Most of the channels were not blocked by iron oxide nanoparticles (Fig. 2b). XRD pattern of Mag-SBA-15 shows that major phase of magnetite or maghemite was mixed with minor phase hematite (Fig. 2c). Unreacted iron salts with propionic acid might be converted to hematite during high temperature treatment under air [31]. The physical properties of Mag-SBA-15 were characterized by N_2 sorption isotherms. The N_2 isotherm is typical for type IV mesoporous materials (Fig. 2d). The surface area was 297 $m^2\,g^{-1}$, which was reduced compared with pure SBA-15 silica (~500 $m^2\,g^{-1}$) due to increased weight of iron oxide nanoparticles (~36 wt% Fe_2O_3). The average pore size, determined from adsorption isotherms, was 6.7 nm (Fig. 2e).

Mag-OMC was synthesized by using SBA-15 and pyrrole as a template and a carbon source, respectively. After the oxidative polymerization of pyrrole, Fe^{2+} ions were converted to magnetic nanoparticles in the carbon pores. A typical TEM image of Mag-OMC reveals that the magnetic nanoparticles were embedded in the carbon walls (Fig. 3). The pore size and BET surface area of Mag-OMC were 2.9 nm and 643 $m^2\,g^{-1}$, respectively. Magnetic mesoporous carbon materials were typically synthesized via a multi-step synthesis [40], starting with the separate synthesis of magnetic nanoparticles. The magnetic mesoporous carbon with open pores in this work (Mag-OMC) was synthesized via a simpler synthetic procedure. The Fe^{2+} ions were used as a catalyst for the pyrrole polymerization, and converted to magnetic nanoparticles embedded in the carbon walls, thus leading to magnetic mesoporous carbon with open pores [36]. The present work is the first demonstration of its potential uses as an adsorbent for the removal of environmental contaminants.

3.2. Recovery and repetitive utilization of magnet sorbent materials

The recovery of particles was investigated by iterative magnetic capture (Fig. S1 in supplementary data) and release using a magnet in aqueous solution. By using a magnet, most particles of Mag-SBA-15 were recovered within 60 min while the recovery of Mag-OMC was slower than Mag-SBA-15 by showing the capture of about 90% particles within 60 min. Fig. 4 shows repeated magnetic capture and release of Mag-SBA-15 and Mag-OMC. Mag-SBA-15 were recovered by magnetic capture within 60 min, and then suspended again. After 10 cycles, it was observed that there was no significant loss of Mag-SBA-15 (Fig. 4). However, the recovery of Mag-OMC was reduced as the number of cycles increased, and 79% of initial Mag-OMC remained after 10 cycles because Mag-OMC could not be fully recovered within 60 min. To improve the recovery rate, the time for magnetic capture could be extended, a different geometry employed (i.e. directed flow over magnet surface), or a stronger external magnetic field could be employed. We also envision that the amount of incorporated magnetic nanoparticles can be increased for a quicker magnetic separation.

3.3. Mercury(II) adsorption

Prior to conducting the actual Hg(II) adsorption experiments, we measured the kinetics of Hg(II) adsorption on the thiol functionalized Mag-SBA-15 at pH 5.0 and ionic strength condition of I = 0.01 M $NaNO_3$. The results of these preliminary kinetic tests showed the fractional Hg(II) adsorption uptake (%) as a function of contact time (Fig. 5a). The Hg(II) adsorption was rapid during the initial contact time, and then slowed down gradually as the equilibrium condition was approached. Hg(II) adsorption reached a steady-state condition after 7 h with an uptake of approximately 97%, which remained same for the duration of 24 h contact time. Based on these preliminary kinetic results, all of the subsequent batch equilibrium adsorption experiments were carried out with one day of contact time.

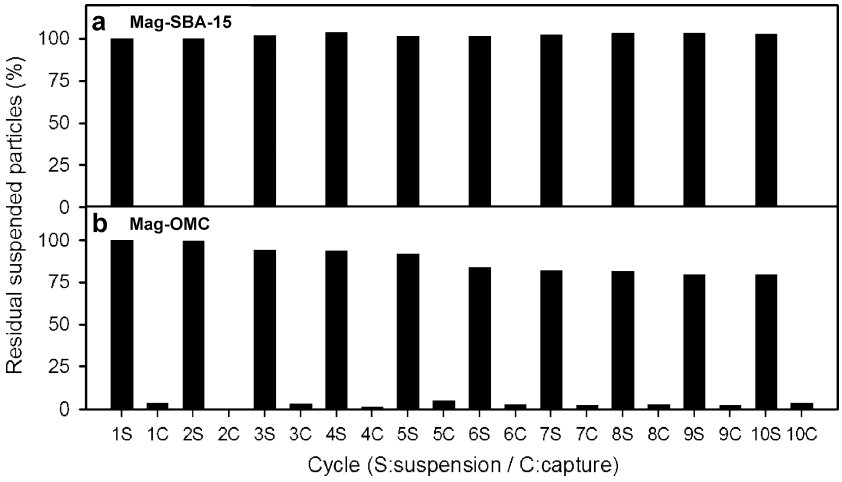

Fig. 4. Cyclic recovery of porous magnetic nanoparticles: (a) Mag-SBA-15; (b) Mag-OMC.

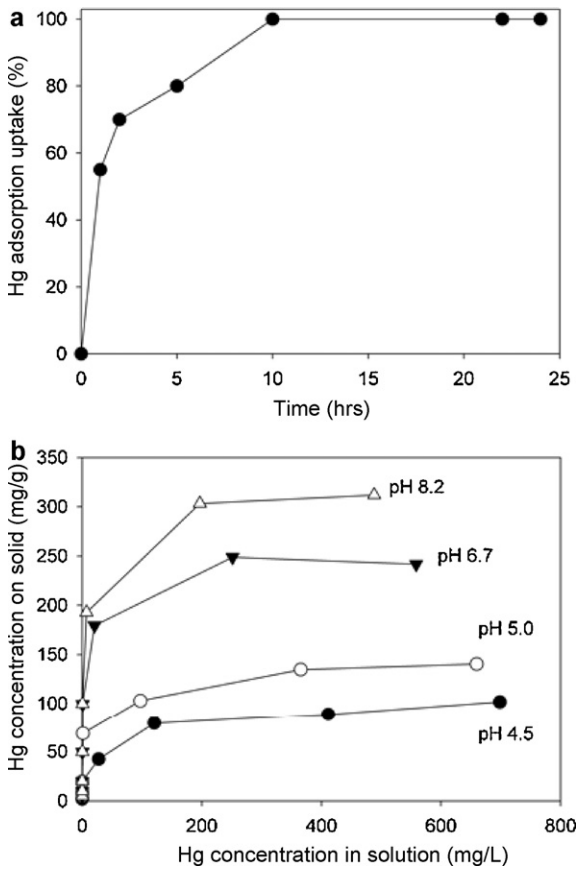

Fig. 5. (a) Hg(II) adsorption on thiol functionalized Mag-SBA-15 as a function of time using $I = 0.01$ M $NaNO_3$ background electrolyte with an initial Hg(II) concentration of 2 mg L^{-1} at pH 5.0; (b) Hg(II) adsorption isotherms on thiol functionalized Mag-SBA-15 at pH values of 4.5, 5.0, 6.7 and 8.2.

The subsequent batch experiments were conducted using various initial Hg(II) concentrations at different pH's. The Hg(II) adsorption isotherms are shown in Fig. 5b. Hg(II) adsorption to thiol-functionalized Mag-SBA-15 showed high affinity at low initial Hg(II) concentrations. Because mercury is characterized as a "soft" Lewis acid and it forms strong covalent bonds with "soft" Lewis bases like the thiol group, a high Hg(II) adsorption affinity on the thiol group of Mag-SBA-15 is noticeable, especially at low initial Hg(II) concentrations [32]. The relatively low Hg(II) uptake at low pH of 5.0 compared to the uptake at higher pH of 8.5 can be attributed to competition with the hydrogen ions at the lower pH condition. The Hg(II) isotherm was fitted by Langmuir isotherm model:

$$Q = Q_{max}\frac{bC}{1+bC} \quad (1)$$

where Q is Hg(II) concentration on the adsorbents (mg g^{-1}); Q_{max} is the maximum Hg(II) concentration on the adsorbents (mg g^{-1}); b is a Langmuir constant; and C is Hg(II) concentration in the solution (mg L^{-1}). The maximum Hg(II) removal capacity (Q_{max}) was determined by linearized Langmuir equation, and the fitted parameters are shown in Table 1. The distribution coefficients (K_d) were calculated at the low concentration range of the Langmuir isotherm. Higher K_d value was obtained at the higher pH condition, which is consistent with the electrostatic binding of Hg(II) due to the presence of deprotonated surface adsorption sites.

Table 1
Parameters for Langmuir and linear isotherms.

pH	Langmuir isotherm parameters			Linear isotherm parameters	
	b	Q_{max} (mg g^{-1})	R^2	K_d (mL g^{-1})[a]	R^2
4.5	1.1	90.9	0.98	107.8	0.99
5.0	0.56	188.7	0.99	109.5	0.99
6.7	0.51	333.3	0.99	150.4	0.99
8.2	1.0	357.1	0.99	281.9	0.99

[a] Distribution coefficient (K_d) was determined at low concentration data in Langmuir isotherm.

3.4. Dye adsorption

Another exemplary application of porous magnetic nanoparticles as adsorbents was investigated by using Mag-OMC for the adsorption of a fluorescent dye, fluorescein, from aqueous solution. When 40 mg of Mag-OMC was added to 10,000 ppm of fluorescein solution and rigorously shaken, the color of solution was changed from green to colorless within minutes. It indicates that the fluorescent dye was quickly and strongly adsorbed into Mag-OMC. The fluorescent dye-loaded Mag-OMC could be separated by using a magnet (Fig. 6). The fluorescent intensity was totally disappeared after 60 min mixing and 40 min magnet separation. The black particles of Mag-OMC could be attached to the magnet, the clear solution could be easily decanted off or removed by a simple manipulation such as pipetting. This result demonstrates that Mag-OMC has magnetic property and can potentially be used as a magnetic adsorbent to remove dyes or other hydrophobic pollutants from the liquid phase for the wastewater treatment processes.

3.5. Tyrosinase entrapped Mag-SBA-15

As a model case for the application of magnetic mesoporous materials in a recyclable biocatalyst for biodegradation, we immobilized tyrosinase (TY) in Mag-SBA-15. TY is an oxidative enzyme that can be used for the oxidation and remediation of harmful phenol compounds. To add vales on this approach, we adopted the approach of nanoscale enzyme reactors to stabilize the TY activity, which consists of two simple steps: enzyme adsorption and crosslinking [41–43]. In other words, TY was adsorbed into Mag-SBA-15, and further crosslinked to prepare the nanoscale enzyme reactors of TY (NER-TY), which can stabilize the TY activity by preventing the TY leaching and denaturation [41–43]. As a control, we also prepared adsorbed TY (ADS-TY) in Mag-SBA-15 without enzyme crosslinking, and compared the stabilities of ADS-TY and NER-TY in the TY-catalyzed oxidation of catechol. The initial activ-

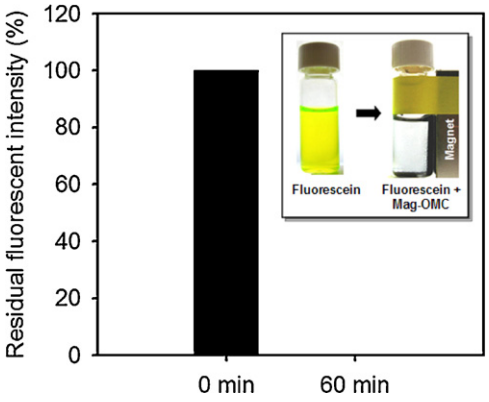

Fig. 6. Residual fluorescent intensity of fluorescein in aqueous solution before and after 60 min adsorption by Mag-OMC. Inset indicates fluorescein solution (left) and adsorption of the fluorescein on Mag-OMC and recovery of the fluorescein loaded Mag-OMC by using a magnet (right).

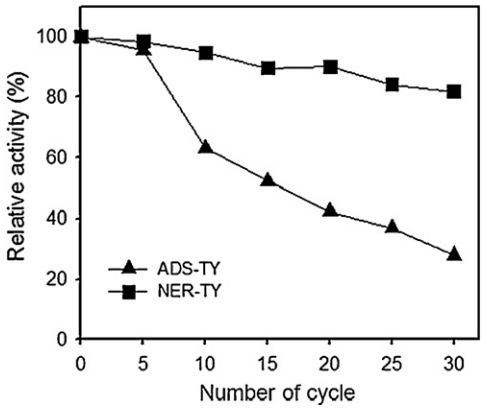

Fig. 7. Stabilities of ADS-TY and NER-TY at room temperature under rigorous shaking in cycles of magnetic separation and excessive washing. One cycle consists of magnetic separation, replenishment of solution, and excessive washing for 1 h. The residual activity was measured after every five cycles, and the relative activity represents the ratio of residual activity to the initial activity of each sample.

ity of ADS-TY and NER-TY were 0.052 and 0.250 A392 min^{-1} per mg of Mag-SBA-15, respectively, which can be explained by higher enzyme loading of NER-TY than ADS-TY due to the prevention of enzyme leaching [42]. To investigate the leaching of TY from Mag-SBA-15, the ADS-TY and NER-TY samples were incubated under rigorous shaking condition (250 rpm), and the residual TY activity was measured after every five cycles of magnetic capture, replenishment of solution, and excessive washing. ADS-TY showed a gradual loss of TY activity, which can be attributed to a continuous leaching of TY during iterative washing and magnet separation. On the other hand, NER-TY showed the stabilized TY activity during excessive washing and magnetic separation. For example, 82% of initial activity was preserved after 30 iterative cycles of activity measurements and washings with NER-TY (Fig. 7). The stability of free tyrosinase was also checked as a control, and the activity of free tyrosinase decreased very rapidly (Fig. S2 in supplementary data) even under incubation with no cycle of magnetic separation and excessive washing. This result suggests that NER-TY is stable due to negligible leaching of TY from Mag-SBA-15 and prevention of TY denaturation by multi-point covalent linkages on the surface of TY molecules. This impressive stability of crosslinked enzyme in mesoporous silica will enable their repeated uses with an easy recycle for real enzyme applications in various fields such as bioremediation, environmental monitoring, and enzymatic synthesis.

4. Conclusions

It has been demonstrated that magnetically separable mesoporous silica and carbon materials can be successfully synthesized into formats viable for a range of chemical separations. We have shown they can be used as recoverable adsorbents for inorganic and organic environmental contaminants and recyclable biocatalytic scaffolds for biodegradation. Although mesoporous materials showed high efficiencies in removal of contaminants, the efficient recovery of adsorbents after usage is a very important issue in real applications. By incorporating iron oxide nanoparticles, magnetic mesoporous materials can achieve not only effective adsorption but also efficient recovery property. The structural, chemical and biological stabilities of magnetic mesoporous materials make them good candidates for a wide range of solid phase separation and biodegradation applications. Therefore, magnetic-separable mesoporous materials would have a significant impact on adsorbent-based chemical processes and environmental remediation/cleanup efforts.

Acknowledgements

Portions of this work were supported by grants from the National Research Foundation (NRF) funded by the Korean Ministry of Education, Science & Technology (MEST) (2009-0082314, 2009-0084771, and K20902001448-10E0100-03010), the Seoul R&BD Program (10920), and by grant from the Korea Institute of Science & Technology (2E22181). This work was also supported by the Pacific Northwest National Laboratory Directed Research Program. The research was performed in part at the W. R. Wiley Environmental Molecular Sciences Laboratory, a national scientific-user facility sponsored by the U.S. Department of Energy's Office of Biological and Environmental Research and located at the Pacific Northwest National Laboratory.

Appendix A. Supplementary data

Supplementary data associated with this article can be found, in the online version, at doi:10.1016/j.jhazmat.2011.06.022.

References

[1] D.M. Hamby, Site remediation techniques supporting environmental restoration activities—a review, Sci. Total Environ. 191 (1996) 203–224.
[2] R.J. Watts, Hazardous wastes: sources, pathways, and receptors, John Wiley and Sons, Inc., 1997.
[3] M.D. LaGrega, P.L. Buckingham, J.C. Evans, Hazardous waste management, McGraw-Hill, Inc., 1994.
[4] Q.L. Lu, G.A. Sorial, Adsorption of phenolics on activated carbon – impact of pore size and molecular oxygen, Chemosphere 55 (2004) 671–679.
[5] N.A. Zeid, G. Nakhla, S. Farooq, E. Oseitwum, Activated carbon adsorption in oxidizing environments, Water Res. 29 (1995) 653–660.
[6] R.V. Siriwardane, M.S. Shen, E.P. Fisher, Adsorption of CO_2 on zeolites at moderate temperatures, Energy Fuels 19 (2005) 1153–1159.
[7] M.A. Hernandez, L. Corona, A.I. Gonzalez, F. Rojas, V.H. Lara, F. Silva, Quantitative study of the adsorption of aromatic hydrocarbons (benzene, toluene, and p-xylene) on dealuminated clinoptilolites, Ind. Eng. Chem. Res. 44 (2005) 2908–2916.
[8] B.H. Gu, J. Schmitt, Z. Chen, L.Y. Liang, J.F. McCarthy, Adsorption and desorption of different organic matter fractions on iron oxide, Geochim. Cosmochim. Acta 59 (1995) 219–229.
[9] C.T. Yavuz, J.T. Mayo, W.W. Yu, A. Prakash, J.C. Falkner, S. Yean, L.L. Cong, H.J. Shipley, A. Kan, M. Tomson, D. Natelson, V.L. Colvin, Low-field magnetic separation of monodisperse Fe_3O_4 nanocrystals, Science 314 (2006) 964–967.
[10] L.A. Belyakova, N.N. Vlasova, L.P. Golovkova, A.M. Varvarin, D.Y. Lyashenko, A.A. Svezhentsova, N.G. Stukalina, A.A. Chuiko, Role of surface nature of functional silicas in adsorption of monocarboxylic and bile acids, J. Colloid Interface Sci. 258 (2003) 1–9.
[11] C.T. Kresge, M.E. Leonowicz, W.J. Roth, J.C. Vartuli, J.S. Beck, Ordered mesoporous molecular-sieves synthesized by a liquid–crystal template mechanism, Nature 359 (1992) 710–712.
[12] J.S. Beck, J.C. Vartuli, W.J. Roth, M.E. Leonowicz, C.T. Kresge, K.D. Schmitt, C.T.W. Chu, D.H. Olson, E.W. Sheppard, S.B. Mccullen, J.B. Higgins, J.L. Schlenker, A new family of mesoporous molecular-sieves prepared with liquid-crystal templates, J. Am. Chem. Soc. 114 (1992) 10834–10843.
[13] J.Y. Ying, C.P. Mehnert, M.S. Wong, Synthesis and applications of supramolecular-templated mesoporous materials, Angew. Chem. Int. Ed. 38 (1999) 56–77.
[14] F. Schuth, Endo- and exotemplating to create high-surface-area inorganic materials, Angew. Chem. Int. Ed. 42 (2003) 3604–3622.
[15] P.T. Tanev, M. Chibwe, T.J. Pinnavaia, Titanium-containing mesoporous molecular-sieves for catalytic-oxidation of aromatic-compounds, Nature 368 (1994) 321–323.
[16] P.T. Tanev, T.J. Pinnavaia, A neutral templating route to mesoporous molecular-sieves, Science 267 (1995) 865–867.
[17] S.A. Bagshaw, E. Prouzet, T.J. Pinnavaia, Templating of mesoporous molecular-sieves by nonionic polyethylene oxide surfactants, Science 269 (1995) 1242–1244.
[18] D.Y. Zhao, J.L. Feng, Q.S. Huo, N. Melosh, G.H. Fredrickson, B.F. Chmelka, G.D. Stucky, Triblock copolymer syntheses of mesoporous silica with periodic 50 to 300 angstrom pores, Science 279 (1998) 548–552.
[19] S.V. Mattigod, X.D. Feng, G.E. Fryxell, J. Liu, M.L. Gong, Separation of complexed mercury from aqueous wastes using self-assembled mercaptan on mesoporous silica, Sep. Sci. Technol. 34 (1999) 2329–2345.
[20] W. Yantasee, Y.H. Lin, G.E. Fryxell, B.J. Busche, J.C. Birnbaum, Removal of heavy metals from aqueous solution using novel nanoengineered sorbents: self-assembled carbamoylphosphonic acids on mesoporous silica, Sep. Sci. Technol. 38 (2003) 3809–3825.

[21] Y.H. Lin, G.E. Fryxell, H. Wu, M. Engelhard, Selective sorption of cesium using self-assembled monolayers on mesoporous supports, Environ. Sci. Technol. 35 (2001) 3962–3966.
[22] G.E. Fryxell, S.V. Mattigod, Y. Lin, H. Wu, S.K. Fiskum, K.E. Parker, F. Zheng, W. Yantasee, T.S. Zemanian, R.S. Addleman, J. Liu, J. Xu, K.M. Kemner, S. Kelly, X. Feng, Design and synthesis of self-assembled monolayers on mesoporous supports (SAMMS): the importance of ligand posture in functional nanomaterials, J. Mater. Chem. 17 (2007) 2863–2874.
[23] W. Yantasee, G.E. Fryxell, R.S. Addleman, R.J. Wiacek, K. Pattamakomsan, V. Koonsiripaiboon, V. Sukwarotwat, J. Xu, K.N. Raymond, Selective removal of lanthanides from natural waters, acidic streams and dialysate, J. Hazard. Mater. 168 (2009) 1233–1238.
[24] P.H.M. Hoet, A. Nemmar, B. Nemery, Health impact of nanomaterials? Nature Biotechnol. 22 (2004) 19–119.
[25] Y. Kim, B. Lee, J. Yi, Preparation of functionalized mesostructured silica containing magnetite (MSM) for the removal of copper ions in aqueous solutions and its magnetic separation, Sep. Sci. Technol. 38 (2003) 2533–2548.
[26] X.Q. Chen, K.F. Lam, Q.J. Zhang, B.C. Pan, M. Arruebo, K.L. Yeung, Synthesis of highly selective magnetic mesoporous adsorbent, J. Phys. Chem. C 113 (2009) 9804–9813.
[27] H. Tian, J.J. Li, Q. Shen, H.L. Wang, Z.P. Hao, L.D. Zou, Q. Hu, Using shell-tunable mesoporous Fe3O4@HMS and magnetic separation to remove DDT from aqueous media, J. Hazard. Mater. 171 (2009) 459–464.
[28] P. Wang, I.M.C. Lo, Synthesis of mesoporous magnetic gamma-Fe_2O_3 and its application to Cr(VI) removal from contaminated water, Water Res. 43 (2009) 3727–3734.
[29] X. Huang, X.P. Liao, B. Shi, Tannin-immobilized mesoporous silica bead (BT-SiO_2) as an effective adsorbent of Cr(III) in aqueous solutions, J. Hazard. Mater. 173 (2010) 33–39.
[30] E.A. Pinheiro, P.P. Deabreu, F. Galembeck, E.C. Dasilva, H. Vargas, Magnetite crystal-formation from iron(iii) hydroxide acetate – an electron-spin-resonance study, Langmuir 3 (1987) 445–448.
[31] A.B. Bourlinos, M.A. Karakassides, A. Simopoulos, D. Petridis, Synthesis and characterization of magnetically modified clay composites, Chem. Mater. 12 (2000) 2640–2645.
[32] A. Bourlinos, A. Simopoulos, D. Petridis, H. Okumura, G. Hadjipanayis, Silica-maghemite nanocomposites, Adv. Mater. 13 (2001) 289–291.
[33] A.B. Bourlinos, A. Simopoulos, N. Boukos, D. Petridis, Magnetic modification of the external surfaces in the MCM-41 porous silica: synthesis, characterization, and functionalization, J. Phys. Chem. B 105 (2001) 7432–7437.
[34] X. Feng, G.E. Fryxell, L.Q. Wang, A.Y. Kim, J. Liu, K.M. Kemner, Functionalized monolayers on ordered mesoporous supports, Science 276 (1997) 923–926.
[35] R.M. Grudzien, S. Pikns, M. Jaroniec, Synthesis and properties of ordered mesoporous organosilicas with vinyl and mercaptopropyl surface groups: the effect of ligand concentration on pore structure, J. Phys. Chem. C 113 (2009) 4875–4884.
[36] J. Lee, S.M. Jin, Y. Hwang, J.G. Park, H.M. Park, T. Hyeon, Simple synthesis of mesoporous carbon with magnetic nanoparticles embedded in carbon rods, Carbon 43 (2005) 2536–2543.
[37] L.Z. Wang, J.L. Shi, W.H. Zhang, M.L. Ruan, J. Yu, D.S. Yan, Self-organization of ordered silver nanocrystal arrays on cubic mesoporous silica surfaces, Chem. Mater. 11 (1999) 3015–3017.
[38] H. Kang, Y. Jun, J.I. Park, K.B. Lee, J. Cheon, Synthesis of porous palladium superlattice nanoballs and nanowires, Chem. Mater. 12 (2000) 3530–3532.
[39] A.H. Lu, W.C. Li, A. Kiefer, W. Schmidt, E. Bill, G. Fink, F. Schuth, Fabrication of magnetically separable mesostructured silica with an open pore system, J. Am. Chem. Soc. 126 (2004) 8616–8617.
[40] A.H. Lu, W. Schmidt, N. Matoussevitch, H. Bonnemann, B. Spliethoff, B. Tesche, E. Bill, W. Kiefer, F. Schuth, Nanoengineering of a magnetically separable hydrogenation catalyst, Angew. Chem. Int. Ed. 43 (2004) 4303–4306.
[41] J. Lee, J. Kim, H.F. Jia, M.I. Kim, J.H. Kwak, S.M. Jin, A. Dohnalkova, H.G. Park, H.N. Chang, P. Wang, J.W. Grate, T. Hyeon, Simple synthesis of hierarchically ordered mesocellular mesoporous silica materials hosting crosslinked enzyme aggregates, Small 1 (2005) 744–753.
[42] M.I. Kim, J. Kim, J. Lee, S. Shin, H. Bin Na, T. Hyeon, H.G. Park, H.N. Chang, One-dimensional crosslinked enzyme aggregates in SBA-15: Superior catalytic behavior to conventional enzyme immobilization, Microporous Mesoporous Mater. 111 (2008) 18–23.
[43] K.Y. Kwon, J. Youn, J.H. Kim, Y. Park, C. Jeon, B.C. Kim, Y. Kwon, X. Zhao, P. Wang, B.I. Sang, J. Lee, H.G. Park, H.N. Chang, T. Hyeon, S. Ha, H.-T. Jung, J. Kim, Nanoscale enzyme reactors in mesoporous carbon for improved performance and lifetime of biosensors and biofuel cells, Biosens. Bioelectron. 26 (2010) 655–660.